Chemical control of thermal expansion in cation-exchanged zeolite A

Carey, Thomas; Tang, Chiu C.; Hriljac, Joseph A.; Anderson, Paul A.

DOI:
10.1021/cm403312q

Document Version
Peer reviewed version

Citation for published version (Harvard):
Carey, T, Tang, CC, Hriljac, JA & Anderson, PA 2014, 'Chemical control of thermal expansion in cation-exchanged zeolite A', *Chemistry of Materials*, vol. 26, no. 4, pp. 1561-1566. https://doi.org/10.1021/cm403312q

Chemical Control of Thermal Expansion in Cation-Exchanged Zeolite A.

Thomas Carey[a], Chiu C. Tang[b], Joseph A. Hriljac[*a] and Paul A. Anderson[*a].

[a] School of Chemistry, University of Birmingham, Edgbaston, Birmingham B15 2TT, UK. E-mail: p.a.anderson@bham.ac.uk, j.a.hriljac@bham.ac.uk; Tel: +44 (0)121 414 4447.

[b] Diamond Light Source Ltd, Harwell Science and Innovation Campus, Didcot, Oxfordshire, OX11 0DE, UK.

KEYWORDS: Negative thermal expansion, Zeolite A, LTA structure type.

ABSTRACT: Variable-temperature powder X-ray diffraction studies have been used to monitor dramatic changes in the thermal expansion properties of zeolites with the LTA topology on changing the pore contents. Detailed structural analysis was performed on dehydrated Li-, Na-, K-, Rb- and Cs-exchanged zeolite A, and a comparison made with their purely siliceous analogue ITQ-29. Mean thermal expansion coefficients were also determined for the hydrated alkali-metal-exchanged forms. Thermal expansion behaviour ranging from negative to positive was observed as different monovalent cations were included in the zeolite pores. Cation-induced strain to the zeolite framework has been shown to play a significant role in the thermal expansion mechanism of LTA-zeolites. Atomic-scale mechanisms behind the thermal expansion behavior have been deduced for ITQ-29, dehydrated Ag-A and dehydrated Na-A systems.

Introduction

Materials that exhibit unusual physical properties attract considerable attention in modern day research for their potential application in a wide variety of fields. Negative thermal expansion (NTE) is an extraordinary phenomenon where materials contract in volume on heating (or expand on cooling). Although a familiar property of ice, only a small number of other solids have been shown to display this remarkable thermal behavior including some metal oxides,[1-2] metal cyanides,[3] polymers[4] and zeolites.[5-11] Zeolites are microporous materials that can accommodate a wide variety of cations in their structures. It is important to understand how zeolites behave as a function of temperature as they are used in many commercial applications including petroleum production, pollution control, chemical sensing and gas separation. Extensive research on purely siliceous zeolite structures has been carried out in recent years, which has shown that NTE is the commonly observed thermal behavior for this class of compounds rather than the unexpected.[5-12]

An accepted mechanism for NTE in siliceous zeolites is that correlated structural vibrations take place that do not significantly distort the individual SiO_4 tetrahedra, so-called 'rigid unit modes' (RUMs).[12] Figure 1 illustrates how the cooperative rotation of the corner-linked rigid tetrahedra (shown for only 4 tetrahedra for clarity) about their T–O–T linkages (where T = Si or Al) can result in an overall unit cell volume reduction in zeolites with the LTA topology. Thermal excitation resulting in this vibrational mode becomes more prevalent as energy is introduced into the system. Relatively little attention has been paid to aluminum-containing zeolites where the structures and properties are known to be particularly sensitive to the extra-framework charge-balancing cations and guest molecules in the pores.[13-18] For this reason, it is important to understand what effect changing the contents of the zeolite pores has on its thermal expansion properties. Couves *et al.*[16] reported that zeolite Na-X showed NTE behavior over a sub-ambient temperature range, but no structural details were provided. Other studies on zeolites Ba-Y,[13] HZSM-5,[15] and Pb- and Cd-RHO[14] have shown that varying the water content in the zeolitic pores can have a significant effect on the thermal expansion behavior but these studies did not provide detailed atomistic information and were complicated by dehydration during the course of the high temperature measurements.

In previous work,[18] we investigated the effect of modifying the pore contents of LTA zeolites by studying the dehydrated and hydrated forms of silver zeolite A ($Ag_{96}[Al_{96}Si_{96}O_{384}]wH_2O$), as well as its purely siliceous analogue ITQ-29 ($[Si_{24}O_{48}]$). The LTA structure is composed of β-cages that are linked *via* double 4-rings forming larger α-cages in-between. Three main sites are available in this structure for non-framework cations to occupy: the single 6-ring (S6R), single 8-ring (S8R) and near the double 4-ring (D4R) (figure 1). Dramatic changes in the thermal expansion behavior from strong negative to weak positive were reported as the zeolite pore contents were modified. Detailed structural mechanisms were proposed for the anhydrous structures but not for the hydrated system due to the high degree of disorder in the pore contents.

Here we report an extended investigation into the effect that differently sized monovalent cations have on the thermal expansion behavior of zeolites with the LTA topology by studying the dehydrated and hydrated lithium (Li-), sodium (Na-) potassium (K-), rubidium (Rb-) and caesium (Cs-) exchanged forms of zeolite A. Variable-temperature high-resolution powder X-ray Diffraction (XRD) studies were car-

ried out in a sub-ambient temperature range (100–300 K) to avoid compositional changes arising from dehydration. Previously reported work on the dehydrated Ag-A and ITQ-29 systems are also reviewed in order to set the discussion in context. A long-term objective of this work is to determine the structural mechanisms behind the complex thermal expansion behavior in aluminum-containing zeolites and to establish whether it is possible to tune zeolite materials chemically to produce a desired coefficient of thermal expansion (such as zero) for potential applications.

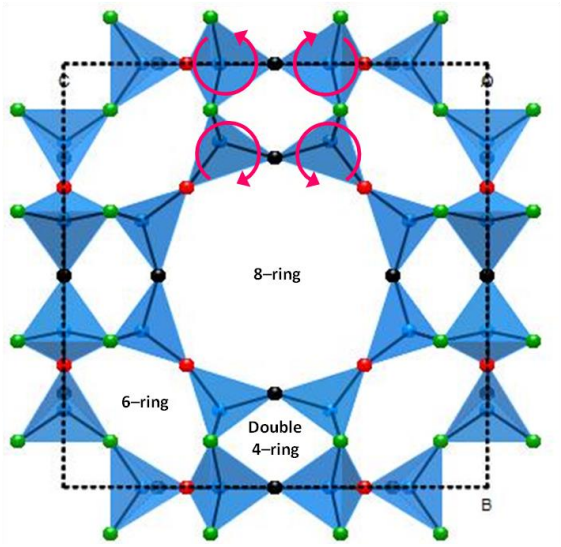

Figure 1 – Representation of the framework of the cubic LTA structure (Si/Al=green, O1 = black, O2 = red and O3 = blue) viewed down [100].

Experimental

Na-A was prepared using the IZA-verified zeolite A preparation.[19] Ion exchange reactions were used to prepare the Li-, K-, Rb- and Cs-forms of zeolite A by stirring Na-A with the appropriate 0.1 mol dm^{-3} nitrate solution under gentle heat (40–50°C) for 24 hours. In order to maximize the degree of ion exchange, this reaction was repeated a number of times as summarized in table 1. Powder XRD was used to check the crystallinity of the exchanged zeolites and XRF analysis for the confirmation of elemental composition. Full cation exchange was not achieved for $Rb_{0.79}Na_{0.21}$-A and $Cs_{0.58}Na_{0.42}$-A, as the crystallinity of the zeolites greatly deteriorated after more than 10 ion exchanges.

Dehydration was achieved by heating the zeolites at 673 K for 12 hours under vacuum (10^{-6} mbar). All dehydrated samples were then stored and prepared for analysis in an argon-filled glove box. Variable-temperature powder synchrotron XRD data were collected at 20 K intervals for dehydrated zeolite A samples on beamline I11 [λ = 0.82741(2) Å] at the Diamond Light Source, UK, using the multi-analyzing crystals (MAC) detector.[20] The wavelength was precisely calibrated using a high quality powder standard of Si (SRM640c). All samples were loaded into 0.5 mm diameter borosilicate glass capillaries and flame-sealed. Pawley[21] and Rietveld[22] refinements were performed using the computer software TOPAS.[23] Zeolite A was indexed in space group $Fm\bar{3}c$ ($a \approx 24$ Å). Thermal parameters of like atoms were grouped in each Rietveld refinement Due to their poor scattering ability, the occupancies of the Li^+ cations were fixed. Successful Rietveld analysis was not possible for any of the hydrated systems due to the high disorder of the zeolite pore contents. Bond valence sums and partial charge values were determined using the methods described by Brown[24] and Sanderson,[25] respectively.

Table 1 – Ion exchange details for the preparation of Li-, Ag-, K-, $(Rb_{0.79}Na_{0.21})$- and $(Cs_{0.58}Na_{0.42})$-A.

Sample	No. of ion exchanges	Calculated unit cell formula from XRF results
Li-A	8	$Li_{92}Na_4(Al_{96}Si_{96}O_{384})$
K-A	8	$K_{93}Na_3(Al_{96}Si_{96}O_{384})$
$Rb_{0.79}Na_{0.21}$-A	10	$Rb_{76}Na_{20}(Al_{96}Si_{96}O_{384})$
$Cs_{0.58}Na_{0.42}$-A	10	$Cs_{56}Na_{40}(Al_{96}Si_{96}O_{384})$

Results

The size and position of the intrapore alkali-metal cations were shown to have a considerable effect on the thermal expansion behaviour of zeolite A. Table 2 details all of the calculated mean coefficients of thermal expansion, $\overline{\alpha_v}_{(100–300\ K)}$, for the dehydrated and hydrated cation-exchanged forms of zeolite A; those of Ag-A and ITQ-29 are also shown for comparison.[18] Weak NTE behaviour was observed for dehydrated Na-A with a $\overline{\alpha_v}_{(100–300\ K)}$ coefficient similar to that of dehydrated Ag-A. This seems consistent with the ionic radii of Na^+ (0.99 Å) and Ag^+ (1.00 Å), which are comparable.[26] More surprisingly, however, weak positive thermal expansion (PTE) was observed for dehydrated Li-A and K-A, and extremely weak NTE behaviour was observed for the dehydrated $Rb_{0.79}Na_{0.21}$-A and $Cs_{0.58}Na_{0.42}$-A systems. PTE behaviour was observed in all the hydrated zeolite A systems studied. Larger $\overline{\alpha_v}_{(100–300\ K)}$ coefficients were determined as the cationic size increased in the fully-exchanged hydrated zeolite A systems, however, smaller $\overline{\alpha_v}_{(100–300\ K)}$ values were calculated for the partly exchanged systems.

Table 2 – Calculated mean volume thermal expansion coefficients from 100 K to 300 K of the LTA systems studied.

LTA System	**Mean Volume Thermal Expansion Coefficient / 10^{-6} K^{-1}**	
	Dehydrated	**Hydrated**
ITQ-29	–22.1	-
Li-A	0.79	16.5
Na-A	–6.34	18.8
Ag-A	–7.68	-
K-A	2.03	32.6
$Rb_{0.79}Na_{0.21}$-A	–0.78	11.9
$Cs_{0.58}Na_{0.42}$-A	–1.76	14.0

Two different cation positions, similar to those reported in the literature,[27-33] were identified for the dehydrated alkali-metal-exchanged zeolite A systems: the S6R and S8R sites. Together these sites can accommodate 88 of the 96 monovalent cations per unit cell necessary to balance the anionic

charge of the framework. A further potential cation site was identified near the D4R units but was not included in refinements owing to very low occupancy (<0.01). Small cations, such as Li^+ and Na^+, were shown to be able to fit in the centre of the S6R and occupy similar cationic positions to those observed in dehydrated Ag-A. In contrast, larger cations such as K^+, Rb^+ and Cs^+, were not able to fit into the S6R and were identified in sites either side of the S6R in the α-cage (S6Rα) or β-cage (S6Rβ), as well as in a more centralized S8R position (figure 2).

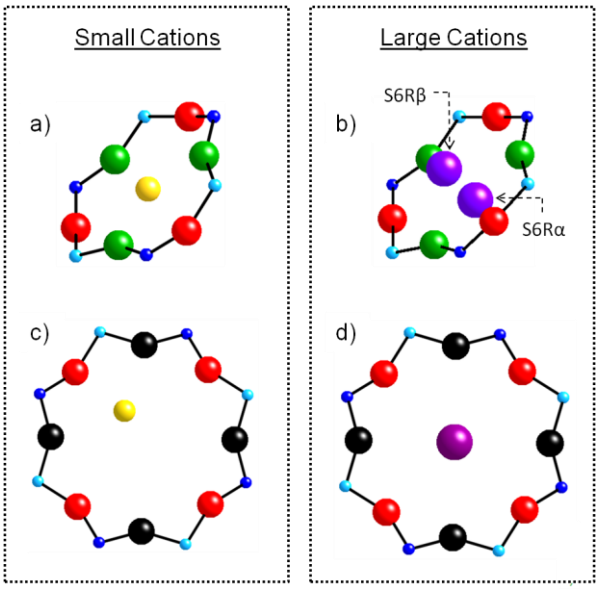

Figure 2 – Positions of the small and large cations in the S6R (a and b) and S8R (c and d) of zeolite A (light blue = Al, dark blue = Si, red = O(2), green = O(3), yellow = small cation and purple = large cation).

Discussion

The effect of exchanging different monovalent cations into zeolite A resulted in varying amounts of strain being put upon the framework as shown in the calculated Si–O–Al and O–T–O bond angles (see supplementary information). This in turn had a huge impact on the thermal expansion behavior as discussed below. Previously,[18] we showed that the strong NTE behavior observed for ITQ-29 is caused by the rotation of rigid SiO_4 tetrahedra. The framework of ITQ-29 bears no net charge, therefore its pores contain no exchangeable cations or guest water molecules. This allows for a direct comparison of the thermal expansion behavior of vacant and occupied LTA frameworks. Significant changes in the Si–O–Si angles were observed upon heating which led to a 0.46 % contraction in the unit cell volume. The Si–O(1)–Si bond angle decreased by 6.39 % on heating causing the O(1) to move towards the centre of the S8R. In contrast, the Si–O(2)–Si and Si–O(3)–Si bond angles both increased by 6.29 % and 1.26 %, respectively, causing O(2) to move away from the centre of the S8R towards the plane of the S6R and O(3) to move towards the centre of the D4R. These changes in the Si–O–Si bond angles indicated that correlated rotation of the rigid tetrahedra upon heating caused the unit cell to contract in volume as shown in figure 3a (crystallographic oxygens have been colour coded for clarity). The Si–O(1)–Si bond angle was shown to play a key role in the thermal expansion behavior of ITQ–29 as it was the only bond angle to decrease in value upon unit cell contraction. This bond angle bridges the D4R (connecting the β-cages) and contracted the Si–O(1)–Si distance by ~1% on heating in ITQ-29.

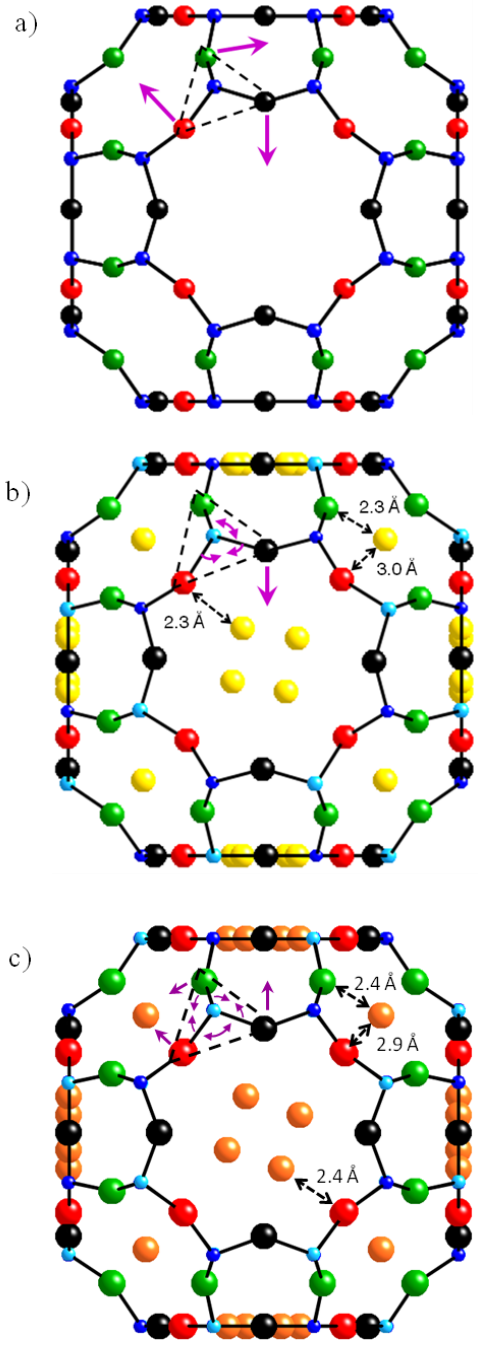

Figure 3 - Single α-cage in a) ITQ-29, b) dehydrated Ag-A and c) dehydrated Na-A down [100] plane illustrating the changes in Si–O–Al and O–T–O bond angles on heating (dark blue = Si, light blue = Al, black = O(1), red = O(2), green = O(3), yellow = Ag^+ and orange = Na^+). Purple arrows indicate movement of atoms upon heating.

Considerable changes in the thermal expansion behavior and mechanism were observed when Ag^+ cations were included in the zeolite pores.[18] Weak NTE behavior was observed

for dehydrated Ag-A with a $\overline{\alpha_{v(100-300\ K)}}$ value of $-7.68 \times 10^{-6}\ K^{-1}$. This equates to a unit cell volume contraction of 0.17 % upon heating, much smaller than that observed in ITQ-29. As shown in figure 3b, the Si–O(1)-Al bond angle decreased on heating as it did in ITQ-29 but by the smaller amount of 3.49 %. However, the Si–O(2)–Al and Si–O(3)–Al angles did not increase, but remained roughly constant over the whole temperature range. Significant distortions in the TO_4 tetrahedra were observed upon heating. The O(1)–T–O(2) angle decreased by ~2.5° upon heating from the ideal value and O(1)–T–O(3) angle increased by ~2°. Taken together, these results suggested that the intrapore Ag^+ cations had an anchoring effect on the framework O(2) and O(3) atoms, which restricted the rotation of the TO_4 tetrahedra on heating. This resulted in a distortion of the tetrahedra and a much smaller contraction ~0.22% of the Si–O(1)–Al distance, mirrored by a considerably reduced overall unit cell contraction compared to ITQ-29. Cations in the S6R site were considered the most likely cause of the anchoring effect.

Despite their similarities in thermal expansion behaviour, table 2, significant differences in the structural mechanism behind the NTE were determined for dehydrated Na-A and Ag-A, (figures 3c and 4). In dehydrated Na-A, the Si–O(1)–Al and Si–O(2)–Al bond angles increased on heating by 2.04% and 1.36%, respectively. In contrast, the Si–O(3)–Al bond angle decreased upon heating by 0.44%. These trends in the Si–O–Al bond angle were completely different to those observed in dehydrated Ag-A and from previous observations, an increase in the Si–O(1)–Al should have resulted in a thermal expansion of the unit cell not a contraction. However, through a closer examination of the O–T–O bond angles, the thermal contraction can be explained. As shown in figure 5 considerable distortions away from the ideal TO_4 tetrahedra were observed at low temperature in dehydrated Na-A. At 100 K, the O(3)–T–O(3) and O(1)–T–O(2) bond angles decreased by ~4.4% and ~2.3%, respectively, from their values at 300 K whereas the O(2)–T–O(3) and O(1)–T–O(3) increased by 1% and 2.2%. Taken together the changes in the Si–O–Al angles and distortions in the TO_4 tetrahedra resulted in a contraction in the Si–O(1)–Al distance by 0.16% and an overall NTE over the whole temperature range.

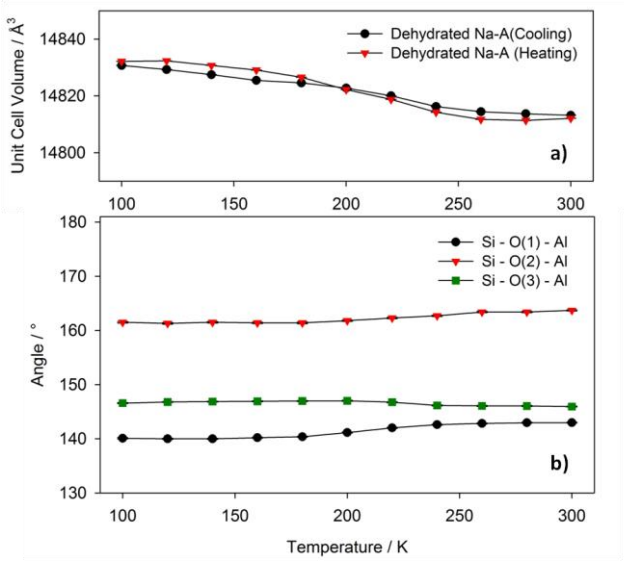

Figure 4 – a) Calculated unit cell volume for dehydrated Na-A from 100–300 K (small error bars at 3σ level, not visible on this scale). b) Si–O–Al bond angles in dehydrated Na-A from 100–300 K (errors at 3σ level).

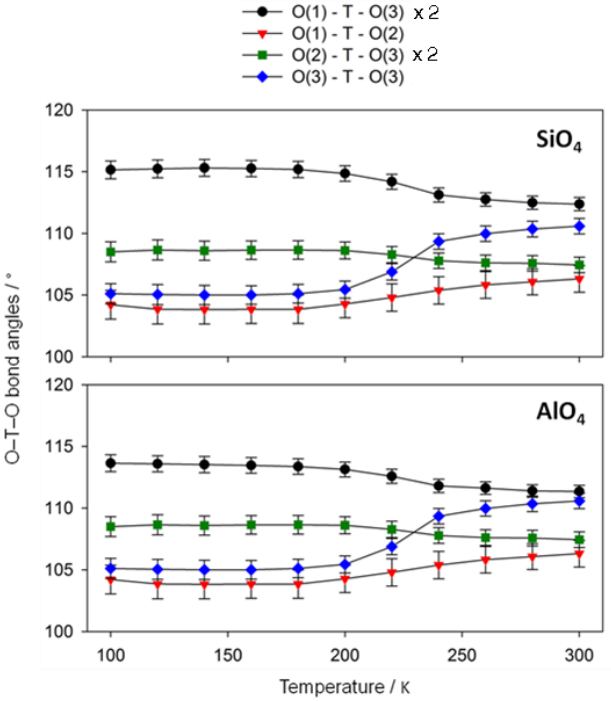

Figure 5 – Calculated O–T–O bond angles for dehydrated Na-A from 100–300 K.

As shown in figure 3c one of the most significant effects of the changes observed on heating dehydrated Na-A was to reduce the Na–O distances of cations in the S6R sites, which did not occur to a significant extent in Ag-A. Although the Na^+ ion is slightly smaller than Ag^+ in coordination numbers greater than four, the very different thermally induced structural changes observed in dehydrated Ag-A and Na-A suggest that the thermal expansion mechanism in zeolite A structures is not solely dependent on the ionic size of the monovalent cations inside the pores. Bond valence sums, atomic partial charges and M^+–O distances were calculated and compared to determine if an electronic contribution also had an effect on the thermal expansion mechanism (tables 3–5). Although relatively little difference in the calculated M^+–O bond distances was observed when dehydrated Na-A and Ag-A were compared, significant differences were determined in the calculated bond valence sums and estimated partial charge values. As shown in tables 4 and 5, slightly higher coordination of the cations was calculated for dehydrated Ag-A as well as a considerably smaller partial charge. This suggests that greater covalency in the Ag^+–O bonds was present in dehydrated Ag-A which may underlie the different thermal expansion mechanisms. At 100 K the tetrahedra in Na-A were significantly distorted and the reduction in distortion on warming from 100–300 K (table 3 and figure 5) could contribute to driving the structural changes observed. In contrast, at 100 K the tetrahedra in Ag-A were relatively undistorted, which may reflect the more covalent bonding and possibly also cluster formation in Ag-A.[34]

Table 3 – Calculated M^+–O bond distances in dehydrated Na-A and Ag-A

M^+– O Bond		Bond Length / Å			
		Ag-A		Na-A	
		300 K	100 K	300 K	100K
S6R	M–O(2)	3.016(9)	3.016(7)	2.936(4)	2.933(3)
	M–O(3)	2.356(6)	2.341(6)	2.349(3)	2.358(3)
S8R	M–O(1)	2.52(1)	2.582(9)	2.43(1)	2.43(1)
	M–O(2)	2.33(2)	2.35(1)	2.49(1)	2.52(1)

Table 4 – Calculated bond valence sums for cations in the 6-ring and 8-ring in dehydrated Ag-A and Na-A at 300 K and 100 K (R_0 = 1.842 for Ag–O and 1.803 for Na–O)

M^+– O Bond		Bond Valence			
		Ag-A		Na-A	
		300 K	100 K	300 K	100 K
S6R	M–O(2) ×3	0.042	0.042	0.047	0.047
	M–O(3) ×3	0.249	0.260	0.229	0.223
Total		0.873	0.906	0.828	0.810
S8R	M–O(1) ×1	0.160	0.135	0.184	0.184
	M–O(2) ×1	0.267	0.253	0.156	0.144
Total		0.427	0.388	0.340	0.328

Table 5 – Calculated partial charge on cations in dehydrated Ag-A and Na-A

Atom	Calculated Partial Charge	
	Ag-A	Na-A
M^+	0.04	0.68

For the remaining anhydrous systems, the general trends in the thermal expansion behavior can be analyzed by plotting the Si–O–Al bond angles vs tilt angle, φ (figure 6). Depmeier[35] first reported this relationship when investigating distortions in the zeolite A framework and defined the tilt angle as the angle between the T–O(1) bond and a plane parallel to the unit cell face:

$$\text{Tilt angle} = \tfrac{1}{2}([\text{Si–O(1)–Al}]° - 109.47°) \qquad (1)$$

As shown in figure 6, clear trends in the Si–O–Al bond angles were observed at 300 K as the size of the cations inside the zeolite framework varied (ITQ-29 has also been included for comparison). A linear increase in the Si–O(1)–Al bond angle was observed as the size of the zeolite cations decreased, whereas a decrease was observed in the Si–O(2)–Al and Si–O(3)–Al bond angles. Through comparing figure 6 with the mean volume thermal expansion coefficients, it can be shown that NTE behavior was only observed in zeolite A when the framework was relatively unstrained (φ = 15–25) i.e. when the Si–O–Al bond angles are similar and the cations are a good fit for the zeolite 6-ring. Even in this region, however, the TO_4 tetrahedra are restricted by coordination to the cations and cannot rotate freely as they can in ITQ-29. This results in distortions to the TO_4 tetrahedra and weaker NTE coefficients.

When larger or smaller cations were included in the pores, greater strain was introduced into the zeolite A framework causing the Si–O–Al bond angles to take more extreme values. In these regions (φ = 5–15 and 25–35) rotations or changes in the geometry of the TO_4 tetrahedra upon thermal excitation appear to be restricted due to cation-induced strain in the framework. This was well illustrated in the dehydrated Li-A and K-A systems where virtually no change in the Si–O–Al and O–T–O bond angles was observed over the whole temperature range (figures 7 and 8). Cations occupying the 6-ring position seemed to have the greatest effect on the framework strain in zeolite A and consequently its thermal expansion behavior. In dehydrated $Rb_{0.79}Na_{0.21}$-A, approximately 69% of the S6R positions were occupied by large Rb^+ cations and an extremely weak NTE coefficient was observed. In dehydrated $Cs_{0.58}Na_{0.42}$-A, only ~38% of the S6R positions were occupied by Cs^+ cations and a larger NTE coefficient was observed. This apparent correlation of thermal expansion coefficient with amount of Na^+ cations in the S6R could in principle provide a means of chemically tuning the coefficient to a desired value or zero.

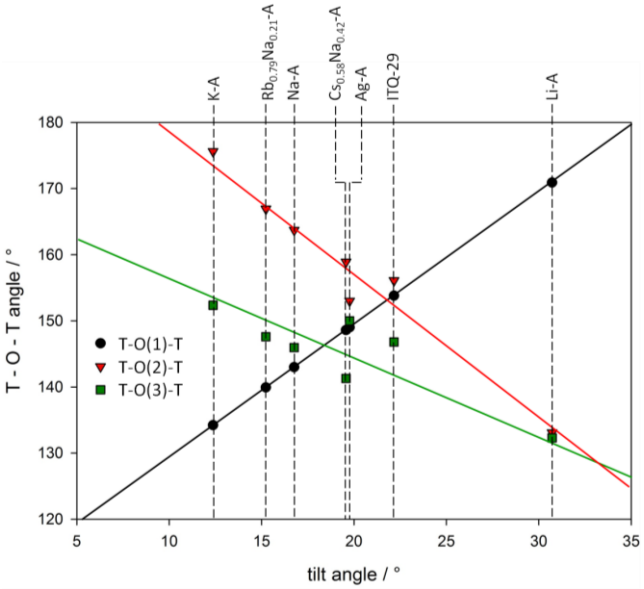

Figure 6 – Graph illustrating the relationship between the T–O–T angles and tilt angles in all of the dehydrated LTA systems at 300 K.

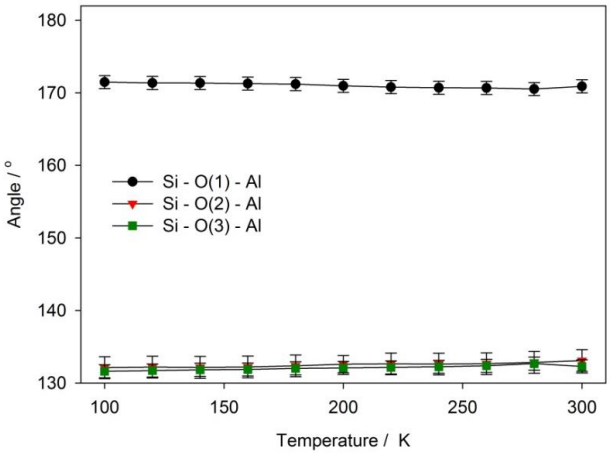

Figure 7 – Calculated Si–O–Al bond angles for dehydrated Li-A from 100–300 K.

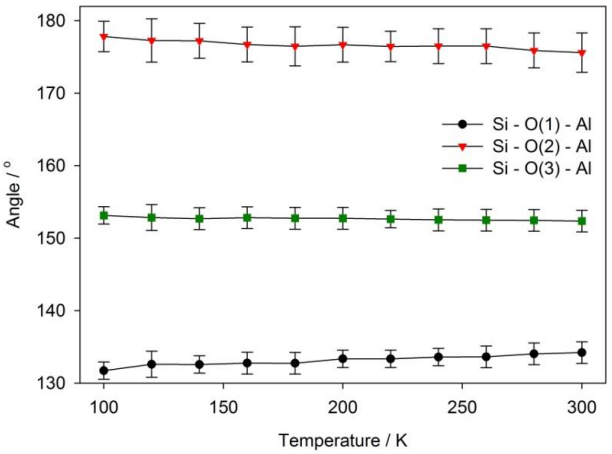

Figure 8 – Calculated Si–O–Al bond angles for dehydrated K-A from 100–300 K.

Conclusions

Strong NTE behavior in the purely siliceous form of the LTA structure, where the pores of the zeolite are vacant, results from rotation of the rigid SiO_4 tetrahedra upon thermal excitation causing a decrease in the zeolite pore volume and an overall contraction of the unit cell. When cations were present in the structure, the rotation of the TO_4 tetrahedra was restricted. Depending upon the size of the cations, different levels of strain were introduced into the zeolite framework. Ideally sized cations such as Ag^+ and Na^+ were able to fit perfectly into the zeolite S6R and caused the least amount of strain. Nevertheless, cation binding caused rotation of the TO_4 tetrahedra to be restricted in dehydrated Na-A and Ag-A resulting in a distortion of the tetrahedra and a weaker NTE coefficient. Cations that were not a good fit for the S6R (such as K^+ and Li^+) introduced much greater strain to the zeolite framework and significantly changed the Si–O–Al bond angles. In these systems significant movement of the TO_4 tetrahedra upon thermal excitation was prevented resulting in weak PTE.

ASSOCIATED CONTENT

Calculated bond lengths and angles of all the samples studied can be found in the supplementary information along with selected Rietveld plots at specific temperature intervals.

ACKNOWLEDGMENT

T.C. was financially supported by the University of Birmingham and Diamond Light Source. We acknowledge the support of Drs Julia Parker and Stephen Thompson for assistance at Diamond. The Siemens D5000 diffractometer was upgraded through Birmingham Science City: Creating and Characterising Next Generation Advanced Materials (West Midlands Centre for Advanced Materials Project 1), with support from Advantage West Midlands and part funded by the European Regional Development Fund.

REFERENCES

(1) Mary, T. A..; Evans, J. S. O.; Vogt, T.; and Sleight, A. W. *Science*, **1996**, 272, 90-92.

(2) Wu, Y.; Kobayashi, A.; Halder, G.J.; Peterson, V.K.; Chapman, K.W.; Lock, N.; Southon, P.D.; Kepert,C.J. *Angew. Chem. Int. Ed.* (2008), 8929-8932.

(3) Goodwin, A. L.; Chapman, K. W.; and Kepert, C. J. *J. Am. Chem. Soc.*, **2005**, 127, 17980-17981.

(4) Maniwa, Y. ; Fujiwara, R.; Kira, H.; Tou, H.; Kataura, H.; Suzuki, S.; Achiba, Y.; Nishibori, E.; Takata, M.; Sakata, M.; Fujiwara, M.; and Suematsu, H. *Phys. Rev. B*, **2001**, 64, 241402.

(5) Woodcock, D. A.; Lightfoot, P.; Wright, P. A.; Villaescusa, L. A.; Díaz-Cabañas, M.; and Camblor, M. A. *J. Mater. Chem.*, **1999**, 9, 349-351.

(6) Woodcock, D. A.; Lightfoot, P.; Villaescusa, L. A.; Díaz-Cabañas, M.; Camblor, M. A.; and Engberg, D. *Chem. Mater.*, **1999**, 11, 2508-2514.

(7) Park, S. H.; Kunstleve, R. W. G.; Graetsch, H.; and Gies, H. *Stud. Surf. Science Catal.* , **1997**, 105, 1989-1994.

(8) Attfield. M. P.; and Sleight, A. W. *Chem. Commun.*, **1998**, 601-602.

(9) Bull, I.; Lightfoot, P.; Villaescusa, L. A.; Bull, L. M.; Gover, R. K. B.; Evans, J. S. O.; and Morris, R. E. *J. Am. Chem. Soc.*, **2003**, 125, 4342-4349.

(10) Villaescusa, L. A.; Lightfoot, P.; Teat, S. J.; and Morris, R. E. *J. Am. Chem. Soc.*, **2001**, 123, 5453-5459.

(11) Lightfoot, P.; Woodcock, D. A.; Maple, M. J.; Villaescusa, L. A.; and Wright, P. A.; *J. Mater. Chem.*, **2001**, 11, 212-216.

(12) Hammonds, K. D.; Heine, V.; and Dove, M. *J. Phys. Chem. B*, **1998**, 102, 1759-1767.

(13) Wang, X.; Hanson, J. C.; Szanyi, J.; and Rodriguez, J. A. *J. Phys. Chem. B*, **2004**, 108, 16613-16616.

(14) Reisner, R. M.; Lee, Y.; Hanson, J. C.; Jones, G. A.; Parise, J. B.; Corbin, D. R.; Toby, B. H.; Freitag, A. Larese, J. Z. and Kahlenberg, V. *Chem. Commun.*, **2000**, 2221-2222.

(15) Jardim, P. M.; Marinkovic, B. A.; Saavedra, A.; Lau, L. Y.; Baehtz, C.; and Rizzo, F. *Micropor. Mesopor. Mater.*, **2004**, 76, 23-28.

(16) Couves, J. W.; Jones, R. H.; Parker, S. C.; Tschaufeser, P.; and Catlow, C. R. A. *J. Phys.: Condens. Matter*, **1993**, 5, 329-332.

(17) Krokidas, P. G.; Skouras, E. D.; Nikolakis, V.;and Burganos, V. N. *J. Phys. Chem. C*, **2010**, 114, 22441-22448.

(18) Carey, T. ; Corma, A.; Rey, F.; Tang, C. C.; Hriljac, J. A.; and Anderson, P. A. *Chem. Commun.*, **2012**, 48, 5829-5831.

(19) Robson, H.; and Lillerud, K. P.; *Verified Syntheses of Zeolitic Materials*, 2nd revised edn., Elsevier, **2001**.

(20) Thompson, S. P.; Parker, J. E.; Potter, J.; Hill, T. P.; Birt, A.; Cobb, T. M.; Yuan, F.; and Tang, C. C. *Rev. Sci. Instrum.*, **2009**, 80, 075107.

(21) Pawley, G. S.; *J. Appl. Cryst.*, **1981**, 357-361.

(22) Rietveld, H. M. *J. Applied Crystallography*, **1969**, 2, 65-71.

(23) Coelho, A. Topas Academic Version 4.1., **2007**

(24) Brown, I. D. *Acta. Cryst.*, **1985**, B41, 244-247.

(25) Sanderson, R. T. *J. Am. Chem. Soc.*, **1983**, 105, 2259-2261.

(26) Ionic coordination in dehydrated zeolites is low therefore values with the lowest commonly available coordination number (CN = 4) were chosen.

(27) Kerr, I. S. Z. *Kristallogr.*, **1974**, 139, 186-189.

(28) Jirak, Z.; Bosacek, V.; Vratislav, S.; Herden, H.; Schollner, R.; Mortier, W. J.; Gellens, L. and Uytterhoeven, J. B. *Zeolites*, **1983**, 3, 255-258.

(29) Reed, T. B.; and Breck, D. W. *J. Am. Chem. Soc.*, **1956**, 78, 5972-5977.

(30) Pluth, J. J.; and Smith, J. V. *J. Am. Chem. Soc.*, **1980**, 102, 4704-4708.

(31) Leung, P. C. W.; Kunz, K. B.; Seff, K.; and Maxwell, I. E. *J. Phys. Chem.*, **1975,** 79, 2157-2162.

(32) Firor, R. L.; and Seff, K.; *J. Am. Chem. Soc.*, **1977**, 99, 1112-1117.

(33) Jr. T. B. V.; and Seff, K. *J. Phys. Chem.*, **1975**, 79, 2163-2167.

(34) Mayoral, A.; Carey, T.; Anderson, P. A.; Axel, L.; and Diaz. I. *Angew. Chem. Int. Ed.*, **2011**, 50, 11230-11233.

(35) Depmeier, W. *Acta Cryst.*, **1985**, B41, 101-108.